# Accepted Manuscript

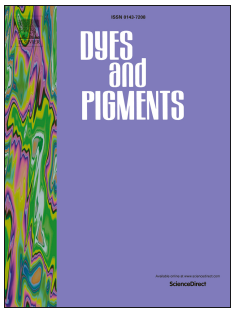


Synthesis of AIE polyethylene glycol-block-polypeptide bioconjugates and cell uptake assessments of their self-assembled nanoparticles

Mingguang Yu, Songjing Zhong, Yusi Quan, Houhe Liu, Junyang Zhong, Xinlin Jiang, Yisi Wang, Guodong Ye, Chunping Ma, Yugang Huang

PII: S0143-7208(19)30916-7

DOI: https://doi.org/10.1016/j.dyepig.2019.107640

Article Number: 107640

Reference: DYPI 107640

To appear in: *Dyes and Pigments*

Received Date: 24 April 2019

Revised Date: 7 June 2019

Accepted Date: 11 June 2019

Please cite this article as: Yu M, Zhong S, Quan Y, Liu H, Zhong J, Jiang X, Wang Y, Ye G, Ma C, Huang Y, Synthesis of AIE polyethylene glycol-block-polypeptide bioconjugates and cell uptake assessments of their self-assembled nanoparticles, *Dyes and Pigments* (2019), doi: https://doi.org/10.1016/j.dyepig.2019.107640.

# Synthesis of AIE polyethylene glycol-block-polypeptide bioconjugates and cell uptake assessments of their self-assembled nanoparticles

Mingguang Yu,[1] Songjing Zhong,[2] Yusi Quan,[2] Houhe Liu,[2] Junyang Zhong,[2] Xinlin Jiang,[2] Yisi Wang,[2] Guodong Ye,[2] Chunping Ma,[3] Yugang Huang,[2,*]

[1] School of Materials Science and Energy Engineering, Foshan University, Foshan 528000, P. R. China

[2] Key Lab of Molecular Target & Clinical Pharmacology of Guangdong Province, School of Pharmaceutical Sciences & the Fifth Affiliated Hospital, Guangzhou Medical University, Guangzhou 511436, P. R. China

[3] School of Materials and Metallurgical Engineering, Guizhou Institute of Technology, Guiyang 550003, P. R. China

*Correspondence to: Dr. Yugang Huang (E-mail: *hyug@gzhmu.edu.cn*)

**ABSTRACT**

A synthetic polypeptide-based bioconjugate bearing tetraphenylethylene (TPE) at the polypeptide side chains, named mPEG-PPLGgTPE, was synthesized by ring-opening polymerization (ROP) of $\alpha$-amino acid-*N*-carboxyanhydride (NCA) along with post-polymerization modification method. Interestingly, the bioconjugate enabled both the aggregation induced emission (AIE) effect at 469 nm and the aggregation caused quenching (ACQ) effect around 365 nm depending on water fraction in the tetrahydrofuran /water (THF/$H_2O$) mixed solution, and this feature was very different from the commonly used TPE-based AIE polymers. The strong emission at the 365 nm was a rarely seen monomeric emission for the TPE units. Further studies on the fluorescence spectra indicated that the monomeric emission was not related with the secondary structure of polypeptides, but caused by the TPE unit itself. The mPEG-

PPLGgTPE could self-assemble to AIE nanoparticles (NPs) in water in a mean size of 253 nm with polyethylene glycol (PEG) as the shells in surface. In addition, HeLa cell uptake level of the NPs was unsatisfactory according to the cell imaging results, which was independent of the polypeptides conformation, the PEG length and the the size of NPs.

*Keywords:* Aggregation induced emission, synthetic polypeptide, aggregation caused quenching, monomeric emission, cell uptake

**1. Introduction**

In recent years, many attentions have been paid to polypeptide-based bioconjugates derived from ring-opening polymerization (ROP) of *α*-amino acid-*N*-carboxyanhydride (NCAs) because of their specific applications in biomedical fields [1]. The attractive applications of these kinds of polymeric materials benefit from continuous improvements in synthetic methods of side-chain functionalized polypeptides [2]. Particularly in anticancer drug delivery, these improvements make these functionalized bioconjugates sensitive to physiological conditions to tumor microenvironment [3-5], which enables the nanocarriers to deliver the drugs into targeted sites in a fashion of passive targeting or active targeting. To get desired biomedical values in use, generally there are two ways to obtain the side-chain modified synthetic polypeptides. One is the functional monomer route, where side-chain modified (SCM) NCA monomers are polymerized, and another one is the post-polymerization modification (PPM) route, where functional molecules are chemically coupled with the reactive polypeptide side-chains [2]. In contrast with the SCM method, using the PPM route to introduce functional groups onto polypeptide side chains has some advantages because many functional groups, for example, the commonly used -$NH_2$, -OH and –COOH groups, will interfere the polymerization of the SCM monomers according to the ROP mechanism so that they are difficult to incorporate into the SCM NCAs [6]. The PPM route depends

on polymerizing first inert NCA monomers containing reactive groups to get the reactive side-chains. Nowadays, complete functionalization of the side-chains in the next step of the PPM route is always desired, so the most attractive idea for the PPM route is to make the side chains "clickable". Hence, various "clickable" groups, including alkyne, alkene and azide groups have been introduced into the polypeptide side chains in the past 10 years [2]. Then, the functional molecules are chemically conjugated to the side chains *via* copper-catalyzed azide-alkyne Huisgen 1, 3-dipolar cycloaddition (CuAAc) [7-11], thiol-yne [12-13] and thiol-ene [14-18] click reactions during the post-polymerization modification step.

Over the past decade, aggregation-induced emission (AIE) nanoparticles (NPs) formed by polymer-based materials are found to be distinctive in biomedical applications because structure, composition, self-assembly morphology and even biological functions of the polymers are tunable in a more ingenious way than that of the traditional organic dyes and quantum dots (QDs) [19]. The AIE characteristic means that dye molecules present strong emissions when they transform themselves from isolated states to aggregated states, which was first reported by Tang in 2001 [20]. The AIE dyes are more popular than the traditional organic dyes in bioimaging and drug delivery [21], since the molecular aggregation of the latter often induces emission quenching effect, a phenomenon resulting from formation of non-emissive energy transfer due to the aggregation of dye molecules [22]. Tetraphenylethylene (TPE), a model AIE molecule, has been incorporated into various amphiphilic polymers to obtain self-assembled NPs to visualize living cells, image and deliver drugs for the tumor therapy. But the AIE polymeric NPs containing TPE are often prepared from polyacrylates and polystyrene-based amphiphilic polymers, because the TPE unit can be easily introduced into the polymerizable acrylate and styrene monomers [23-26]. Nevertheless, the NPs of synthetic polypeptide-based AIE bioconjugates bearing TPE units are rarely seen in the previous reports. Hong *et al.* prepared a tetraphenylthiophene based AIE polypeptide

of poly (γ-benzyl-L-glutamate) [27], but the tetraphenylthiophene located at chain terminal, and this polymer was not amphiphilic. Scarcity of this synthetic polypeptide-based AIE polymer is normal, because incorporating of the TPE molecules into inert SCM NCAs along with purification of NCA monomers is harsh. Therefore, the PPM route depending on polymerizable NCA monomers having reactive groups will be a better choice.

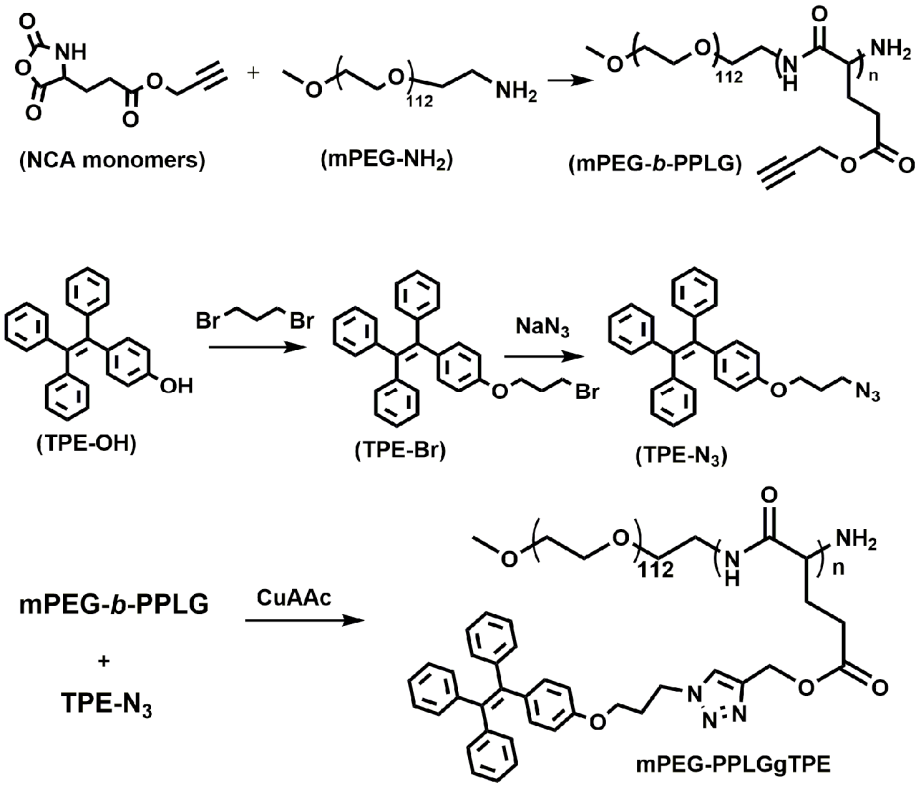


**Scheme 1**. Representative way to synthesize AIE polyethylene glycol-block-polypeptide containing TPE

In this work, a bioconjugate of polyethylene glycol-block-poly (γ-propargyl-L-glutamate) (mPEG-PPLG) was synthesized by the ROP of γ-propargyl-L-glutamate NCA (PLG-NCA) with the methoxypolyethylene glycol amine (mPEG-$NH_2$) as a macroinitiator. Then, the PPLG side chains were modified with an azide of (2-(4-(3-azidopropoxy)phenyl)ethene-1,1,2-triyl)tribenzene (TPE-$N_3$) in a post-polymerization way through the CuAAc reaction, which was illustrated in Scheme 1 with the targeted bioconjugate

designated by mPEG-PPLGgTPE. The PPLG was selected as the post-polymerization precursor as it was easy to access polypeptides with subsequent side chain thiol-yne and CuAAc modifications [7-8, 11-12, 28]. Then, the AIE characteristics of the mPEG-PPLGgTPE were studied in detail by fluorescence spectra. In addition, features for the synthetic polypeptides are their unique α-helical and β-sheeted secondary structure, which is very different from those commonly used polymers mentioned above. Hence, it will be very interesting to understand the polypeptide "conformation–cell imaging" relationship and the "nanoparticle structure–cell imaging" relationship by evaluating the cell uptake level of the obtained AIE NPs.

**2. Experimental section**

*2.1 Materials*

Methoxypolyethylene glycol amine (mPEG-$NH_2$, $M_n$ = 5000 g/mol, 95%) and anhydrous N, N-dimethyl formamide (DMF, 99.8%) were both purchased from J&K and used as received. Glutamic acid (99%), $CuSO_4 \cdot 5H_2O$ (99.5%), sodium ascorbate (99.5%) and 1, 3-dibromopropane (99%) were all purchased from Aladdin Reagent (China) and used without further purification. Propargyl alcohol (99%) and $NaN_3$ (99%) was supplied by Xiya Reagent (China). Fetal bovine serum (FBS), DMEM and PBS buffer used for cell culture were all purchased from Gibco (USA). 3-(4, 5-Dimethylthiazol-2-yl)-5-(3-carboxymethoxyphenyl)-2-(4-sulfophenyl)-2H-tetrazolium inner salt (MTS) was supplied by Sigma-Aldrich (USA). HeLa cells were kindly supplied by Professor. Yi Zhou at the School of Pharmaceutical Sciences of Guangzhou Medical University.

*2.2 Synthesis of propargyl-glutamate and NCA monomers*

The γ-propargyl-L-glutamate (PLG) and γ-propargyl-D,L-glutamate (PDLG) was synthesized according to an improved method reported in our previous work [12, 28]. Briefly, glutamic acid (10.0 g, 0.068 mol)

was suspended in propargyl alcohol (24.8 g, 0.44 mol) in an ice-salt bath. Then sulfuric acid (8.2 g, 98%) was added dropwise over 15 min. After that, the esterification reaction proceeded at room temperature for 3 days. Triethylamine (12.0 g) was added into the mixture to precipitate the crude product, and then isopropyl alcohol (200 mL) was added to dilute the mixture. The precipitate was filtrated and washed by isopropyl alcohol. The wet precipitate was recrystallized in isopropyl alcohol/$H_2O$ (3:1, v/v, 10 mL of isopropyl alcohol used for 1.0 g of wet precipitate). The γ-propargyl-glutamate was finally obtained as white plates. Yields: 41%. $^1$H NMR (400 MHz, $D_2O$, δ): 2.10 (dm, 2H, *CH*$_2$CH$_2$CO), 2.49 (t, 2H,CH$_2$*CH*$_2$CO), 2.80 (t, 1H, COOCH$_2$*C≡CH*), 3.65 (t,1H, *CH*CH$_2$CH$_2$CO), 4.63 (d, 2H, COO*CH*$_2$C≡CH). HR-MS: calcd. [M+K] 225.190, found. 225.196.

PLG-NCA and PDLG-NCA was synthesized according to an improved method in our previous work [12, 28]. Typically, PLG (3.0 g, 0.016 mol) was suspended in anhydrous ethyl acetate (120 mL) in a two-necked flask with a reflux condenser and $N_2$ bubbler. After heating to 70 °C, triphosgene (1.64 g, 55 mmol) was added and the mixture was heated for 45 min. The mixture was then heated to 85 °C and refluxed for 4 h under $N_2$. The solution was cooled to room temperature, filtrated and washed with ice-cold water (150 mL), ice-cold 0.5 % of $NaHCO_3$ solution (150 mL) and ice-cold water (150 mL). The organic phase was then dried by anhydrous $MgSO_4$ and evaporated to obtain PLG-NCA as clear oil. Yields: 40-55 %. $^1$H NMR (400 MHz, $CDCl_3$, δ): 2.18 (dm, 2H, CH*CH*$_2$CH$_2$COO), 2.52 (t, 1H, *C≡CH*), 2.60 (t, 2H, CHCH$_2$*CH*$_2$COO), 4.44 (t, 1H, *CH*CH$_2$CH$_2$COO), 4.69 (d, 2H, COO*CH*$_2$C≡CH), 6.98 (s, br, 1H, -NH- in ring). NCAs monomers are well-known sensitive to moisture and alkali, so mass spectra analysis were not made. The PLG-NCA and PDLG-NCA were directly used for the polymerization in the next step as soon as possible.

*2.3 Synthesis of polyethylene glycol-block-poly(γ-propargyl-L or DL-glutamate) (mPEG-PPLG and mPEG-PPDLG)*

The ROP of PLG and PDLG-NCA monomers initiated by mPEG-$NH_2$ was typically described as follows: NCA monomers (0.53 g, 2.5 mmol) were dissolved into anhydrous DMF (1.0 mL) at room temperature, and then the solution was slowly added into anhydrous DMF (4.0 mL) containing mPEG-$NH_2$ (0.63 g, 0.126 mmol) with a syringe. The resulting solution was stirred for 3 days under dry $N_2$. The resulting solution was added into ether to precipitate the polymer. Yields: 70-85 %.

*2.4 Synthesis of (2-(4-(3-azidopropoxy)phenyl)ethene-1,1,2-triyl)tribenzene (TPE-$N_3$)*

The synthetic route to TPE-$N_3$ was described in the Scheme 1, and the reaction was carried out according to a literature procedure [29-30]. The H NMR spectra were the same as the literature reported.

First, 2-bromo-1,1,2-triphenylethene (4.0 g, 11.93 mmol), (4-hydroxyphenyl)boronic acid (2.0 g, 14.3 mmol), tetrabutylammonium bromide (TBAB, 0.15 g, 0.46 mmol), 2M of $K_2CO_3$ (15 mL) and dioxane (30 mL) were mixed together under $N_2$, and then palladium (0) tetratriphenyl phosphate (50 mg) was added. Under $N_2$, the mixture was stirred for 24 h at 90 °C. After that, the mixture was poured into water and extracted by ethyl acetate three times (60 mL × 3). The organic phase was collected and dried by $Na_2SO_4$. The TPE-OH was purified by column chromatography. Yields: 72 %. $^1$H NMR (400 MHz, $CDCl_3$, δ): 6.63 (2H, d, proton in aromatic ring adjacent to –OH), 6.90-7.10 (17H, m, protons in aromatic rings), 1.29 (s, -OH); HR-MS: calcd. [M-1] 347.450, found. 347.144. IR (KBr, $cm^{-1}$): *v* = 3450 (-OH).

Next, TPE-OH (1.57 g, 4.51 mmol), $K_2CO_3$ powder (1.55 g, 11.2 mol) and 30 mL of acetone were mixed together. Then 1,3-dibromopropane (3.64 g, 18 mmol) was slowly added, and the resulting mixture was refluxed for 24 h at 60 °C. After that, the $K_2CO_3$ was filtrated and washed by 10 mL of acetone. The collected solution was removed by rotary evaporation, and the residues were dissolved in ethyl acetate (120 mL), washed twice by water (50 mL × 2) and then dried by $MgSO_4$. The ethyl acetate was removed

under rotary evaporation, and finally the crude (2-(4-(3-bromopropoxy)phenyl)ethene-1,1,2-triyl)tribenzene (TPE-Br) was purified by column chromatography (cyclohexane/ethyl acetate, 50/1). Yields: 51 %. $^1$H NMR (400 MHz, $CDCl_3$, δ): 6.60-7.20 (m, 19H, protons in aromatic rings), 3.55 (t, 2H, Br*CH$_2$*-), 2.28 (m, 2H, $BrCH_2$*$CH_2$*-), 4.13 (br, 2H, $BrCH_2CH_2$*$CH_2$*O-). HR-MS: calcd. [M+1] 470.420, found. 470.121.

Finally, TPE-$N_3$ was obtained by substitution reaction of TPE-Br with $NaN_3$. Briefly, mixture of TPE-Br (1.87 g, 4.0 mmol), $NaN_3$ (0.90 g, 13.9 mmol) and 60 mL of DMF was refluxed for 24 h at 85 °C. After that, the DMF was removed under rotary evaporation, and then 100 mL of ethyl acetate was added. The organic phase was washed twice by water (30 mL × 2) and dried by $MgSO_4$. The solvent was removed by rotary evaporation, and finally the product was purified by column chromatography with cyclohexane/ethyl acetate as eluent (50/1). Yields: 50 %. $^1$H NMR of TPE-$N_3$, (400 MHz, $CDCl_3$, δ: 6.40-7.40 (m, 19H, protons in aromatic rings), 1.27 and 1.43 (br, 2H, $N_3$*$CH_2$*-), 2.06 (m, 2H, $N_3CH_2$*$CH_2$*-), 3.53 (t, 2H, $N_3CH_2CH_2$*$CH_2$*O-). HR-MS: calcd. [M+1] 431.540, found. 431.204. IR (KBr, cm$^{-1}$): *v* = 2099 (-$N_3$).

*2.5 Grafting TPE-$N_3$ onto the polypeptides*

A typical grafting reaction of mPEG-*b*-PPLG was given as follows: mPEG-*b*-PPLG (0.20 g, 0.28 mmol of alkyne), TPE-$N_3$ (0.145 g, 0.34 mmol of azide) and $CuSO_4 \cdot 5H_2O$ (91 mg, 0.36 mmol) were mixed in DMSO (6.0 mL). The mixture was bubbled with $N_2$ for 20 min and then sodium ascorbate (78 mg, 0.39 mmol) was added. After bubbling $N_2$ for another 10 min, the reaction solution was sealed and stirred for 48 h at 50 °C. The resulting mixture was purified by dialysis (3500 cutoff) against water to remove the excess sodium ascorbate. During the dialysis, EDTA was added to remove the copper salt. After lyophilization, the obtained solid was dissolved in THF, passed through aluminium oxide column to remove copper salt residues, and finally precipitated in cyclohexane to remove the unreacted TPE-$N_3$. Yields: 32 %.

*2.6 Measurements*

NMR spectra were recorded on a Bruke AVANCE III HD 400 MHz spectrometer and $CF_3COOD/CDCl_3$ (1/4, v/v) was used as solvent for the polymers containing polypeptide blocks; Size exclusion chromatography (SEC) was performed on a Malvern Viscotek TDA305max with DMSO containing 20 mM of LiBr as eluent. The measurement was carried out at 50 °C with a flow rate of 0.5 mL/min. The size exclusion was made with an Iguard column and a connected I-Oligo column, Pullulan as standard sample. The signals were collected with a refractive index detector; FTIR spectra were read on a Thermo Nicolet 6700 spectrophotometer and scanned 32 times with a resolution of 2 $cm^{-1}$ by KBr disk method; UV-visible absorption spectra were studied by Agilent 8453 spectrophotometer with $THF/H_2O$ as solvent. The AIE effect was recorded by Fluorescence spectra (FL) on a Shimadzu RF-5301PC spectrometer with a slit width of 3.0 nm and an excitation wavelength ($\lambda_{ex}$) of 330 nm or 365 nm. The polymer was first dissolved in the THF with a given concentration. Then, water was slowly added under a ultrasonic clearer to make sure that the water content was increasing from 0 to 95 % (v %) with a polymer concentration of 0.05 mg/mL; The AIE properties of the blocked polypeptides grafted by TPE was studied by recording the FL of their micellar water solutions. The micellar solution was prepared by first dissolving the AIE polymers in dimethyl sulfoxide (DMSO) with a concentration of 0.20 mg/mL and then dialyzing the polymers against distilled water for 24 h. The water was exchanged every 4 h and finally the nanoparticles (NPs) solution was diluted to 0.10 mg/mL before the test; Dynamic light scattering (DLS) was used to determine size and zeta potential of the NPs on a Malvern Nano-ZS/ZEN-3600 Zetasizer. Three sets of measurements were performed for each sample. The micellar sample was prepared as the same as the AIE determinations mentioned above; Transmission electron microscopy (TEM) observation was performed on a JEM-2010 system. A drop of the micellar solution mentioned

above was deposited on carbon coated copper grids for 1.5 min, and then the water was removed with a piece of filter paper.

*2.7 Cytotoxicity assay*

The cytotoxicity of the AIE-NPs for HeLa cells was assayed by using MTS cell viability test. Cells were seeded in 96-wells plates at 6000 cells/well and grown for 24 h at 37 °C, 5% $CO_2$ in DMEM medium containing 10% FBS, 1% penicillin and streptomycin. After removing the medium, the AIE NP solution was added into the wells, and then DMEM was added to dilute the solution into desired concentration. After that, the cells were incubated at 37 °C for 24 h again. Then, 20 μl of MTS was added into the cells in each well and the plates were incubated for additional 2 h. The OD values were then recorded at the wavelength of 490 nm using a microplate reader (Biotek). For each sample, 4 times were repeated at each concentration.

*2.8 Cell uptake*

The cell imaging ability of the AIE NPs for the HeLa cells was evaluated with a Nikon ECLIPSE 80i confocal laser scanning microscopy (CLSM) with an excited wavelength of 405 nm and a Leica DMi8 fluorescence microscope. Cells were seeded in culture dishes and grown for 24 h. After that, the given solutions of AIE NPs in DMEM culture were added into each dish. After incubation for 4 h, the cells with internalized AIE NPs were washed by PBS three times before the microscope observation. Flow cytometry (Beckman) determination was also performed to investigate the cell uptake of the AIE NPs, and the cells were cultured similar to the CLSM observations.

**3. Results and discussion**

*3.1 Synthesis and characterization*

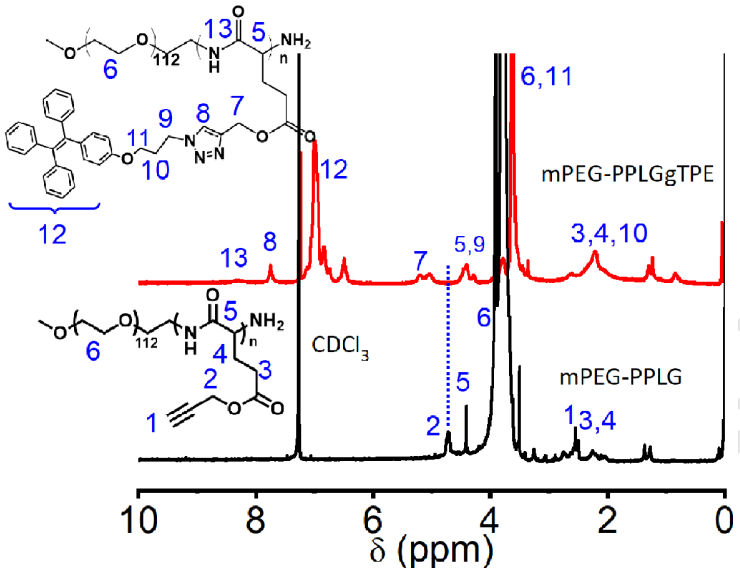


**Figure 1.**[1] H NMR spectra of mPEG-PPLG in $CDCl_3/CF_3COOD$ (4/1, v/v) and mPEG-PPLGgTPE in $CDCl_3$.

The synthesis of AIE bioconjugate of mPEG-*b*-PPLGgTPE was given in the Scheme 1. First, mPEG-block-poly(propargyl-L-glutamate) naming mPEG-PPLG was synthesized by the ROP of the PLG-NCA monomer with mPEG-$NH_2$ as an initiator. Then, TPE was grafted onto the polypeptide blocks by the CuAAc coupling reaction, and the obtained polymer was denoted by mPEG-PPLGgTPE. Structures of all the resulting polymers were characterized by the $^1$H NMR in Figure 1, where peak assignments were also made. Because length of the mPEG ($M_n$ = 5000 g/mol) blocks had been known, the length of PPLG with a degree of polymerization (DP) of 9.0 was calculated according to area ratio of peak 2 and peak 6 in the Figure 1. Thus, the obtained copolymer was denoted by mPEG-$PPLG_9$. The structure of the mPEG-*b*-PPLGgTPE in the final step was also confirmed by the $^1$H NMR spectra. The peak assignments showed that the side-chain –$CH_2$– protons of peak 2 was shifted from 4.70 to 5.10 ppm (peak 7) after the CuAAc coupling reaction, and no residual signal of the peak 2 at 4.70 ppm was observed after the grafting reaction. These results indicated that the TPE was successfully grafted onto the polypeptide side chains with a nearly complete grafting efficiency. A distinct peak at 7.75 ppm (peak 8) assigned to resulting

triazole ring also proved to be the high grafting efficiency of the CuAAc reaction, so the obtained polymer was denoted by mPEG-PPLG$_9$gTPE.

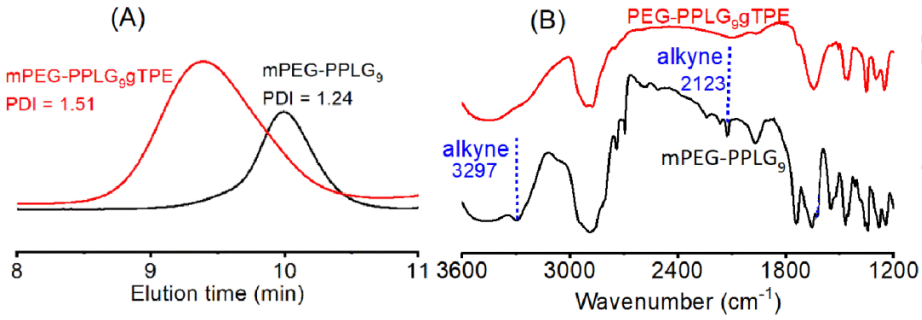


**Figure 2.** (A) SEC traces of the mPEG-PPLG$_9$ and the mPEG-PPLG$_9$gTPE in DMSO; (B) FTIR spectra of the mPEG-PPLG$_9$ and the mPEG-PPLG$_9$gTPE.

The polymers as prepared were further characterized by SEC in DMSO, which was given in Figure 2A. It can be seen that molecular weight ($M_w$) of the mPEG-PPLG$_9$gTPE was bigger than that of the mPEG-PPLG$_9$, indicating that the TPE molecules were grafted onto the polypeptides successfully. In addition, determined polydispersity index (PDI) was 1.24 for the mPEG-PPLG$_9$ and 1.51 for the mPEG-PPLG$_9$gTPE. FTIR spectra of the mPEG-PPLG$_9$ and the mPEG-PPLG$_9$gTPE in solid were shown in Figure 2B, where the mPEG-PPLG$_9$ showed typical absorption of the alkynes at the 2123 and 3297 cm$^{-1}$. After the CuAAc reaction, the obtained mPEG-PPLG$_9$gTPE the two absorption bands were absent in the Figure 2B, also indicating that the grafting efficiency was high.

*3.2 Absorption and fluorescence properties*

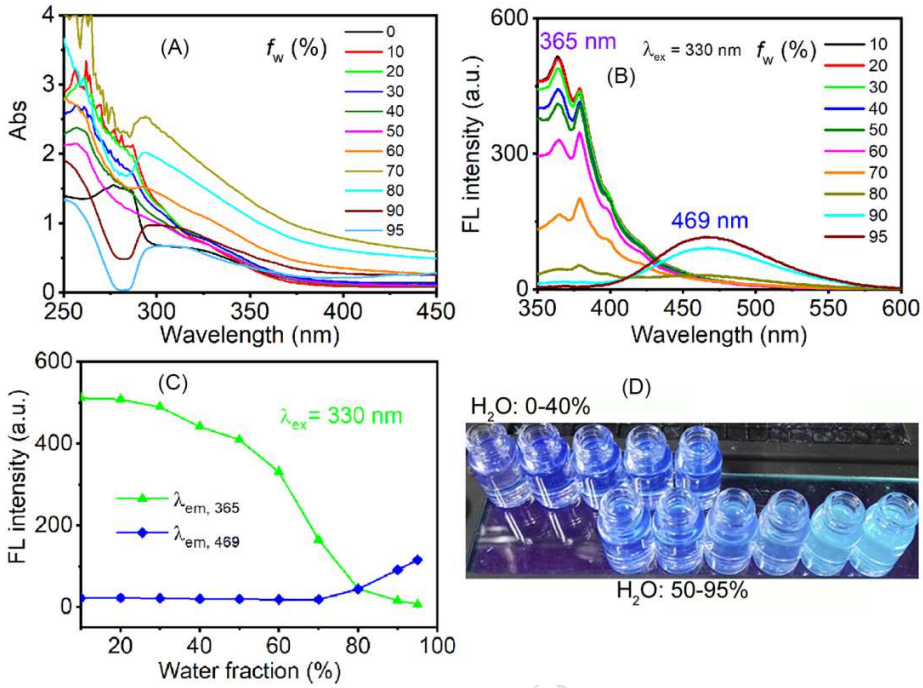


**Figure 3.** (A) UV absorption spectra of the mPEG-PPLG$_9$gTPE (0.05 mg/mL) in THF/$H_2O$; (B) FL spectra of the mPEG-PPLG$_9$gTPE (0.05 mg/mL) with increasing water fraction in the THF/$H_2O$, $\lambda_{ex}$ = 330 nm; (C) Intensity of maximum emission wavelength ($\lambda_{em}$) with increasing water fraction, $\lambda_{ex}$ = 330 nm; (D) Digital photos of the mPEG-PPLG$_9$gTPE in THF/$H_2O$ under a hand-hold UV-lamp ($\lambda_{max}$ = 302 nm).

The UV-vis absorption spectra (Figure 3A) of the mPEG-PPLG$_9$gTPE in THF/$H_2O$ mixture were performed to reveal the aggregate emergence when the water fraction ($f_w$, V %) was increaing from 0 to 95 %. As seen in the Figure 3A, the mPEG-PPLG$_9$gTPE showed a maximum of absorption peak ($\lambda_{max}$) around 280 nm and a shoulder peak at 310 nm in the pure THF. As the $f_w$ exceeded 40 %, the absorption spectra was broader in a red shift, indicating that a Mie effect of light scattering was caused by the nanosized aggregation formation (as shown in following self-assembly analysis) at higher $f_w$ [31]. Under higher water content, inner cores of the formed NPs would be more and more compact, leading to the absorption of the mPEG-PPLG9gTPE in 70-80 % of $H_2O$/THF higher than that of 90-95 %. FL spectra (Figure 3B) were further used to investigate the AIE feature resullting from the aggregation of the mPEG-PPLG$_9$gTPE. As indicated by the Figure 3B, a fluorescence in the range of 350

to 400 nm centered with $\lambda_{em}$ of 365 nm was observed when the $f_w$ was below 70 %. However, this emission vanished and a new emission peak was detected at the $\lambda_{em}$ of 469 nm when the $f_w$ was above 70 %, showing a typical AIE property as a result of the aggregation of the mPEG-PPLG$_9$gTPE. Further, the emission intensity at the $\lambda_{em}$ of 365 and 468 nm was plot *versus* increasing $f_w$ in Figure 3C, where the results clearly indicated that both an aggregation-caused quenching (ACQ) effect and an AIE effect could be seen for this polymer. Actually, a covered blue emission at 416 nm could be revealed when the $\lambda_{ex}$ was changed to be 365 nm (Figure S1). According to the above FL spectra, the mPEG-PPLG$_9$gTPE could emit different color lights from purple to cyan depending on the $f_w$. Thus, visual inspection of the emission colors was presented in the Figure 3D, where a color transfer of purple-blue-cyan was recorded with increasing $f_w$ when the sample was exposed under a UV-lamp. This visual result was consistent with the PL spectra result.

The AIE effect was believed to connect with restriction of intramolecular rotation (RIR ) of TPE units, which inhibited the nonradiative decay and thus led to the aggregation-enhanced emissions [32]. In this work, interestingly, the monomeric emission showing ACQ effect at 365 nm was hard to see in previous literatures. The increasing $f_w$ would enhance the local concentration of TPE units, which means that the concentrated TPE speices enabled the fluorescence quenching as a result of the formation of π-π interaction between phenyl rings. The concentration dependent fluorescence quenching of the monomeric emission for the mPEG-PPLG$_9$gTPE was similar to the typical luminophore of pyrene, which was summarized by *Birks* [33] in his classical photophysics book. The monomeric emission peak of pyrene at 390 nm was decreasing with an enhancing concentration in the concentration region above $10^{-5}$ M, while the peak disappeared until a small and broad emisison without fine bands appeared at the 477 nm in the redder spectral region when the concentration was up to $10^{-1}$ M, a indicator of the emission change from monomeric spieces to excimers [33]. However, the FL spectra of the mPEG-PPLG$_9$gTPE here showed fine emisisons around 365 nm

without any shift upon local concentration increase of TPE units, indicating that this fluorescence came from radiative decay of TPE monomeric spieces, not from the emissions due to the formation of excimers and exciplex [22,33]. As indicated by the Figure 3B, the mPEG-PPLG$_9$gTPE showed the broad bump at 469 nm when the $f_w$ was increased to 90-95%, even though this AIE emisison was not caused by the formation of excimers and exciplex. The reason is that the ACQ effect of TPE monomeric spieces are hardly seen in so many previous literatures until now, and the RIR mechnism proposed by *Tang et al.* [32] can well explain the AIE features of the TPE-based materials at the 469 nm. Hence, further studies on the fluorescence properties of the TPE-$N_3$ will be necessary in the future.

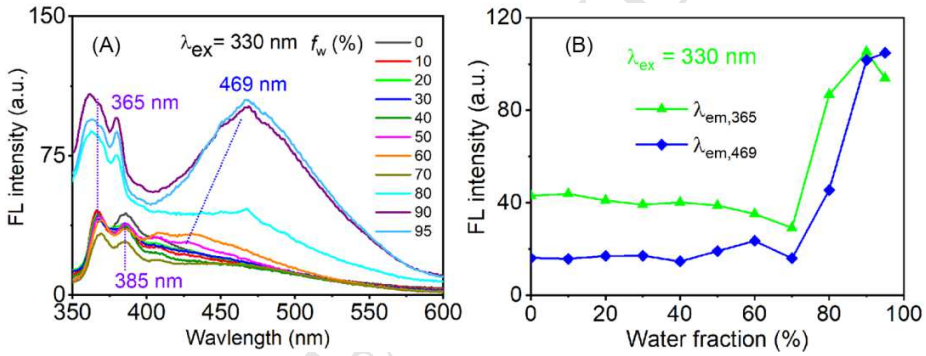


**Figure 4.** (A) FL spectra of the TPE-$N_3$ (0.12 mM) in THF/$H_2O$, $\lambda_{ex}$ = 330 nm; (B) Intensity of maximum emission wavelength ($\lambda_{em}$) with increasing water fraction, $\lambda_{ex}$ = 330 nm.

Particularly, some recent reports indicated that the conformation of the synthetic polypeptides would determine physical and biological properties of these kinds of biomaterials [34]. Thus, there was an interesting speculation whether the secondary structure of the polypeptides determined the unique luminescence property of the mPEG-PPLG$_9$gTPE or not. To testify this, an AIE bioconjugate with racemic polypeptide blocks, denoted by mPEG-PPDLGgTPE, was prepared by the ROP of racemic NCA monomer (PDLG-NCA) ) at the same time. The FL spectra (Figure S2) of this polymer showed the same tendency like the mPEG-PPLG$_9$gTPE when the $f_w$ was rising, suggesting that the

fluorescence of the TPE units was not related with the secondary structure of polypeptides. To gain more insights into the caused monomeric emission of the mPEG-PPLGgTPE, the FL spectra of the TPE-$N_3$ in dilute solution (0.05 mg/mL, 0.12 mM) was scanned with the increasing $f_w$, which was displayed in Figure 4A. Clearly, the FL spectra of TPE-$N_3$ showed one fine monomeric emission at 365 and 385 nm along with a broad bump in the red shift region when the $f_w$ was below 70%. After that, the monomeric emission became stronger and headed towards shorter wavelength reigon when the $f_w$ was high. Additionally, a new bump from 400 to 450 nm appeared as the $f_w$ was increasing. After the $f_w$ exceeded 70%, another broad emission with stronger intensity could be detected at the 469 nm, showing the typical AIE behavior of the TPE again. Figure 4B showed the fluorescence intensity variation as the $f_w$ was increasing. It was found that both the emissions at the 365 nm and 469 nm altered little when the $f_w$ was less than 70%, but the intensity was sharply enhanced after that. Interestingly, the monomeric emission was reduced while the $f_w$ was up to 95%, which means that the fluorescence properties of the TPE-$N_3$ are very similar to that of the pyrene: the increasing local concentration of TPE-$N_3$ can enhance the monomeric emission in the low concentration range, whereas the ACQ effect will happen in concentrated solution if the $f_w$ is close to 100%. To our best knowledges, the strong monomeric emission of the TPE was reported in only three literatures. He *et al.* [35] reported an amphiphilic TPE derivative containing secondary amines to detect wide-range pH alteration in the THF/$H_2O$ mixture. This TPE derivative could show strong monomeric emission at 377 nm at the low pH range, because the resulting electrostatic repulsion between the protonated amines let one molecule not be close to another one to form the π-π interaction between phenyl rings. Zheng *et al.* [36] reported synthesis of a 4-armed star oligo(ethylene glycol) (OEG) with the TPE unit as the core. Once this TPE was included in the cavity of γ-cyclodextrin (γ-CD), the formed complex could show an enhanced monomeric emission at 388 nm. The big cavity of the γ-CD confined the rotation of the phenyl rings of the TPE, which stopped

the formation of π-π interaction and then favored the emissive decay of the excited TPE monomer. Note that this OEGylated TPE was also an amphiphilic TPE derivative. Recently, Lin *et al.* [37] reported a novel photo-switchable polymer bearing TPE moieties within the backbones by the CuAAc reaction. Upon UV-irradiation, the strong monomeric emission of the TPE was found at 385 nm in the THF/$H_2O$ mixture becase of the photo-cyclization happed in the polymer backbone. Chemical structure of all the amphiphilic TPE derivatives mentioned above was complex, however, the hydrophobic TPE-$N_3$ we reported here was the frst TPE-based AIE molecule showing strong monomeric emission in a simpler structure. To further study the effect of functional group on the fluorescence properties of the TPE units, the FL spectra (Figure S3) of the TPE-Br in THF/$H_2O$ were aslo measured. As seen in Figure S3, although the TPE-Br could show the monomeric emission of TPE units in the THF/$H_2O$ when the $f_w$ was less than 70%, its intensity was very weak. The AIE emission of the TPE-Br was very strong when the $f_w$ was high. This result indicated that the TPE-Br is a typical AIE molecule, very different from the TPE-$N_3$. More importantly, this result verfied that the unique monomeric emission of the TPE-$N_3$ was determined by its azide group. Overally, both the mPEG-PPLG$_9$gTPE and the TPE-$N_3$ could display the AIE and the ACQ phenomenon depending on water fraction, and the polypeptide conformation had no effect on the fluorescence properties of the obtained AIE polymers. Thus, it can be concluded that the unique fluorescence behaviors of the mPEG-PPLG$_9$gTPE result only from the TPE units. However, note that the mPEG-PPLG$_9$gTPE showed better AIE ability than that of the TPE-$N_3$, because the effective concentration of TPE molecules in this polymer was much less than that in the TPE-$N_3$. It means that the intramolecular rotation of the TPE phenyl rings was strongly restricted by the polypeptide chains within core of the self-assembled NPs.

*3.3 Self-assembly behaviors*

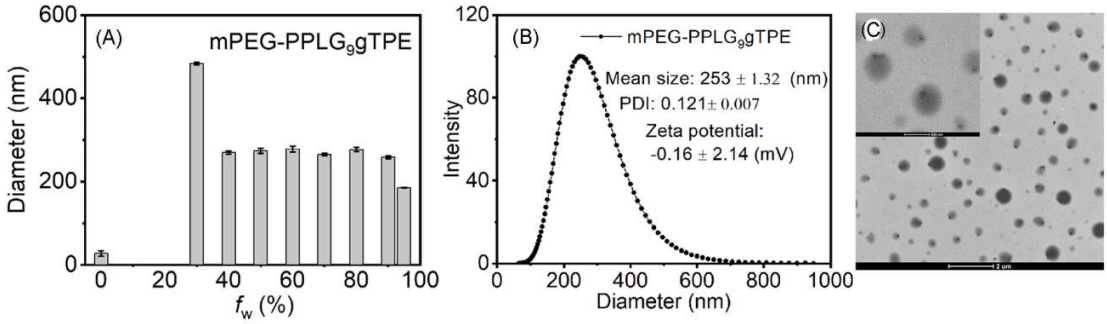


**Figure 5.** (A) DLS results of the mPEG-PPLG$_9$gTPE (0.05 mg/mL) with increasing water fraction in THF/$H_2O$; (B) DLS results of the mPEG-PPLG$_9$gTPE micelles (0.20 mg/mL) in water; (C) TEM image of the mPEG-PPLG$_9$gTPE micelles, and the inset was local amplification of the micelles with a scale bar of 500 nm.

Upon adding water into the THF solution of the mPEG-PPLG$_9$gTPE, aggregation will be formed with increasing water content. Thus, the formation of aggregations and their size changes in the THF/$H_2O$ mixture were measured by DLS, which was displayed in Figure 5A. Interestingly, it was found that the mPEG-PPLG$_9$gTPE can form particles in pure THF with a mean size of 27.3 nm. These particles are probably unimers of the mPEG-PPLG$_9$gTPE because of the large bulk of the grafted TPE units at the side chains and the rigid conformation of the polypeptide blocks. However, the DLS did not give any repeatable and reliable results of the formed particles with the $f_w$ of 10 and 20 %. Above 20%, nano-sized aggregations were formed with decreasing size when the water content was increasing, indicating that the inner cores of the NPs were more and more compact because of closer aggregation of the hydrophobic blocks in the mPEG-PPLG$_9$gTPE.

The mPEG-PPLG$_9$gTPE could self-assemble into NPs in water because of its amphiphilic nature. DLS was still used to determine size of the formed NPs after dialysis, which was seen in Figure 5B. The obtained NPs were in size region of 100 to 600 nm, with an average value of 253 nm and a PDI of 0.121. Additionally, the determined zeta potential was -0.16 mV, close to zero as it was expected, because the coated PEG blocks onto the NP surface were electroneutral. Morphology of the self-assembled NPs was

detected by TEM, and the results in the Figure 5C indicated that the particles were spherical micelles with a slightly broad size distribution, which was identical with the DLS results. The mPEG-PPLG$_9$gTPE NPs could emit bright cyan lights visually in water under a hand-hold UV lamp, and the AIE persistence time was long because more than 60 % of initial emission intensity was remaining after 10 days (Figure S4).

*3.4 Cell uptake assessments*

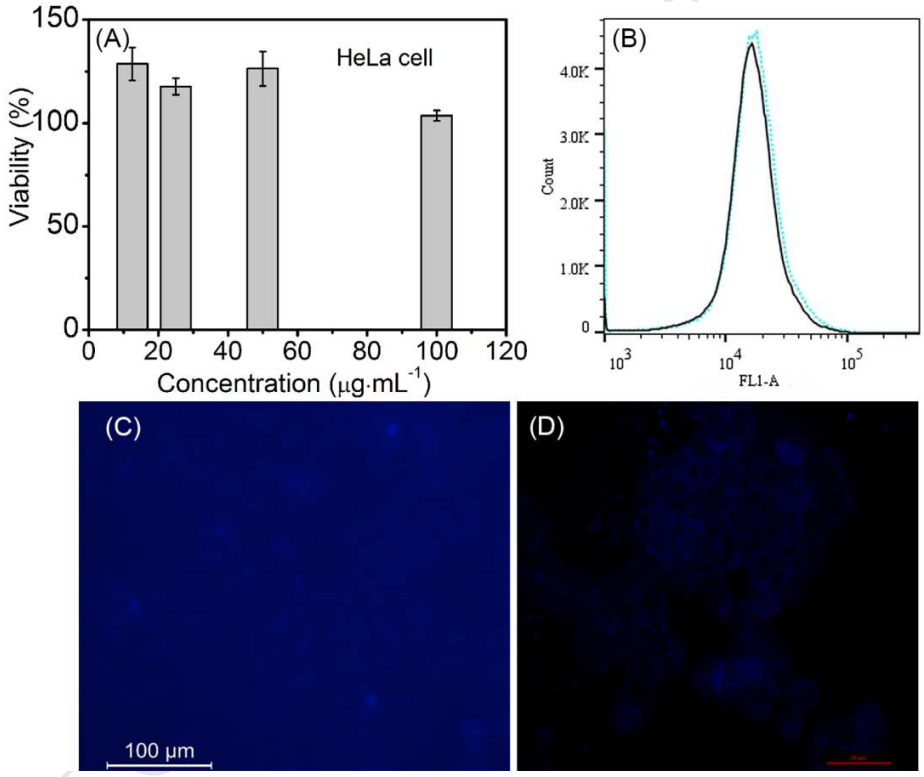


**Figure 6.** (A) Cytotoxicity of the AIE NPs assessed by the MTS assays. (B) Cell uptake of the AIE NPs revealed by flow cytometry. Dot line: HeLa cells uptake of the AIE NPs. Solid line: without any NPs as the control; (C) The CLSM images and (D) fluorescence microscope images of the HeLa cells with the internalized mPEG-PPLG$_9$gTPE NPs.

Cell imaging is a fundamental aspect of the AIE-polymers for use in the biomedical field. Even though various AIE-polymer NPs have been widely used for cell imaging because of their good luminous ability,

many attentions were paid on the acrylate-based and PS-based polymers [19]. However, the synthetic polypeptides are very different from those common polymers because the polypeptide chains are rigid and can adopt α-helical and β-sheeted conformation [34]. Actually, rare synthetic polypeptide-based AIE polymers having TPE units were reported in former researches. As we all know, the strong intramolecular and intermolecular hydrogen bond interactions favor formation of the α-helical and the β-sheeted conformations, and thus studying the cell imaging ability of the mPEG-PPLG$_9$gTPE NPs will be interesting and helpful to understand the structure-function relationship of the synthetic polypeptide-based materials. Herein, the cell uptake ability of the mPEG-PPLG$_9$gTPE NPs was evaluated by the flow cytometry analysis, the fluorescence microscope as well as the CLSM observations. In order to exclude the cytotoxicity effect of the mPEG-PPLG$_9$gTPE, the MTS viability assay was carried out at the same time. Figure 6A showed the HeLa cell viability under different polymer concentration. It can be seen that the mPEG-PPLG$_9$gTPE was non-cytotoxic with the concentration as high as 100 μg/mL. In Figure 6B, the flow cytometry analysis showed that there was nearly no difference between the cells cultured with and without mPEG-PPLG$_9$gTPE NPs, implying that the cell uptake level of the AIE NPs was quite low. Fluorescence microscope was further used to observe the cells internalized with AIE NPs, which was given in Figure 6C. Unfortunately, no clear images of the HeLa cells were gained by the microscope observation, which means that the cell uptake level of the AIE NPs was not high. In Figure 6D, CLSM observation was also made to confirm this, because the CLSM could supply clearer images. As expected, the CLSM made the same result as the fluorescence microscope. Thus, concordant results made by both the flow cytometry analysis and the microscope observations confirmed that the mPEG-PPLG$_9$gTPE NPs were hard to internalize into the cells. Even though reasons leading to that poor cell uptake level are complicated, the influence of structure parameters, including the conformation of the polypeptide and the chain length of the PEG, were studied by the CLSM observations. In this work, the mPEG$_{5k}$-PPDLGgTPE NPs with racemic polypeptide blocks mentioned above and the mPEG$_{2k}$-PPLGgTPE NPs

with shorter PEG chains were both prepared, and their CLSM images of the formed NPs were presented in Figure S5. Similarly, clear images could not be obtained again, which indicated that the conformation of the polypeptides and the PEG chain length could not affect the cell uptake level of the AIE NPs. Particularly, the assembled NPs of $mPEG_{5k}$-PPDLGgTPE was smaller in size than that of the mPEG-$PPLG_9$gTPE NPs (198.9 ± 5.4 nm, DLS results), still showed the poor cell uptake level, indicating that the size of NPs could not determine the cell internalization process, either.

**4. Conclusions**

In summary, a synthetic polypeptide-based AIE bioconjugate consisting of TPE at the polypeptide side chains were synthesized by the post-polymerization modification method. The self-assembled NPs of the amphiphilic bioconjugates could show strong AIE performance. Interestingly, the TPE units in the synthetic polypeptide-based AIE copolymer could show a strong monomeric emission in the THF/water mixture, and thus a color transformation of purple-blue-cyan was seen with the naked eyes. The monomeric emission was independent of the polypeptide conformation. The self-assembled NPs showed poor cell uptake level, which was not determined by the polypeptide conformation, the PEG chain length and the size of the NPs. This work will be helpful to understand the fluorescence characteristic of the TPE units in the synthetic polypeptide-based AIE polymers.

**Acknowledgement**

This work is financially supported by the National Natural Science Foundation of China (51403043), the municipal college research program of Guangzhou education bureau (1201610202) and the High-Level Talent Start-Up Research Project of Foshan University (gg040945).

**Notes**

The authors declare no competing financial interest.

**Appendix A. Supplementary data**

Supplementary data related to this article can be found at: xxxx

**References**

[1] Song Z, Han Z, Lv S, Chen C, Chen L, Yin L, Cheng J. Synthetic polypeptides: from polymer design to supramolecular assembly and biomedical application. Chem Soc Rev 2017;46:6570–6599.

[2] Deming TJ. Synthesis of side-chain modified polypeptides. Chem Rev 2016;116:786–808.

[3] Shen Y, Fu X, Fu W, Li Z. Biodegradable stimuli-responsive polypeptide materials prepared by ring opening polymerization. Chem Soc Rev 2015;44:612–622.

[4] Liu L, Li T, Ruan Z, Yan L. Polypeptide-based artificial erythrocytes conjugated with near infrared photosensitizers for imaging-guided photodynamic therapy. J Mater Sci 2018;53: 9368–9381.

[5] Jing T, Li T, Ruan Z, Yan L. pH and glutathione-stepwise-responsive polypeptide nanogel for smart and efficient drug delivery. J Mater Sci 2018;53:14933–14943.

[6] Hadjichristidis N, Iatrou H, Pitsikalis M, Sakellariou G. Synthesis of well-defined polypeptide-based materials via the ring-opening polymerization of α-amino acid N-carboxyanhydrides. Chem Rev 2009;109:5528–5578.

[7] Xiao C, Zhao C, He P, Tang Z, Chen X, Jing X. Facile synthesis of glycopolypeptides by combination of ring-opening polymerization of an alkyne-substituted N-carboxyanhydride and click "Glycosylation". Macromol Rapid Commun 2010;31:991–997.

[8] Engler AC, Lee HI, Hammond PT. Highly efficient "grafting onto" a polypeptide backbone using click chemistry. Angew Chem Int Ed 2009;48:9334–9338.

[9] Huang J, Habraken G, Audouin F, Heise A. Hydrolytically stable bioactive synthetic glycopeptide homo- and copolymers by combination of NCA polymerization and click reaction macromolecules. 2010;43:6050–6057.

[10] Zhang R, Zheng N, Song Z, Yin L, Cheng J. The effect of side-chain functionality and hydrophobicity on the gene delivery capabilities of cationic helical polypeptides. Biomaterials 2014;35: 3443–3454.

[11] Xiao C, Cheng Y, Zhang Y, Ding J, He C, Zhuang X, Chen X. Side chain impacts on pH- and thermo-responsiveness of tertiary amine functionalized polypeptides. J Polym Sci Part A Polym Chem 2014;52:671–679.

[12] Huang Y, Zeng Y, Yang J, Zeng Z, Zhu F, Chen X. Facile functionalization of polypeptides by thiol-yne photochemistry for biomimetic materials synthesis. Chem Commun 2011;47:7509–7511.

[13] Yi L, Wang Y, Lin G, Lin D, Chen W, Huang Y, Ye G. Synthesis of conformation switchable cationic polypeptides based on poly(S-propargyl-cysteine) for use as siRNA delivery. Int J Biol Macromol 2017;101:758–767.

[14] Sun J, Schlaad H. Thiol-ene clickable polypeptides. Macromolecules 2010; 43:4445–4448

[15] Zhang Y, Lu H, Lin Y, Cheng J. Water-soluble polypeptides with elongated, charged side chains adopt ultrastable helical conformations. Macromolecules 2011;44:6641–6644.

[16] Tang H, Zhang D. Multi-functionalization of helical block copoly(α-peptide)s by orthogonal chemistry. Polym Chem 2011;2:1542−1551.

[17] Zhou J, Chen P, Deng C, Meng F, Cheng R, Zhong Z. A simple and versatile synthetic strategy to functional polypeptides via vinyl sulfone-substituted l-cysteine N -carboxyanhydride. Macromolecules 2013;46:6723−6730.

[18] Krannig KS, Sun J, Schlaad H. Stimuli-responsivity of secondary structures of glycopolypeptides derived from poly(lglutamate-co-allylglycine). Biomacromolecules 2014; 15:978−984.

[19] Zhan R, Pan Y, Manghnani PN, Liu B. AIE polymers: Synthesis, properties, and biological applications. Macromol Biosci 2017;17:1600433.

[20] Luo J, Xie Z, Lam JWY, Cheng L, Chen H, Qiu C, Kwok HS, Zhan X, Liu Y, Zhu D, Tang B. Aggregation-induced emission of 1-methyl-1,2,3,4,5-pentaphenylsilole. Chem Commun 2001; 1740−1741.

[21] Feng G, Liu B. Aggregation-induced emission (AIE) dots: emerging theranostic nanolights. Acc Chem Res

2018;51:1404–1414.

[22] Lakowicz JR. Principles of fluorescence spectroscopy. 3rd ed. Singapore: Springer; 2006.

[23] Li X, Li C, Wang S, Dong H, Ma X, Cao D. Synthesis and properties of photochromic spirooxazine with aggregation-induced emission fluorophores polymeric nanoparticles. Dyes Pigments 2017;142:481-490.

[24] Zhou H, Liu F, Wang X, Yan H, Song J, Ye Q, Tang B, Xu J. Aggregation induced emission based fluorescence pH and temperature sensors: probing polymer interactions in poly(N-isopropyl acrylamide-co-tetra(phenyl)ethene acrylate)/poly(methacrylic acid) interpenetrating polymer networks. J Mater Chem C, 2015;3:5490–5498.

[25] Qi Q, Li Y, Yan X, Zhang F, Jiang S, Su J, Xu B, Fu X, Sun L, Tian W. Intracellular pH sensing using polymeric micelle containing tetraphenylethylene-oxazolidine. Polym Chem 2016;7: 5273–5280.

[26] Ma H, Qi C, Cheng C, Yang Z, Cao H, Yang Z, Tong J, Yao X, Lei Z. AIE-active tetraphenylethylene cross-Linked N-isopropylacrylamide polymer: A long-term fluorescent cellular tracker. ACS Appl Mater Interfaces 2016;8:8341–8348.

[27] Li S, Lin Y, Kuo S, Chuang W, Hong J. Aggregation induced emission enhancement in relation to the secondary structures of poly(g-benzyl-L-glutamate) containing a fluorescenttetraphenylthiophene moiety. Polym Chem 2012;3:2393–2402.

[28] Huang Y, Luo W, Ye G. Synthesis, characterization, conformation and self-assembly behavior of polypeptide-based brush with oligo (ethylene glycol) side chains. J Mole Struct 2015;1081:274–280.

[29] Xu B, He J, Liu Y, Xu B, Zhu Q, Xie M, Zheng Z, Chi Z, Tian W, Jin C, Zhao F, Zhang Y, Xu J. High-performance two-photon absorption luminophores: large action cross sections, free from fluorescence quenching and tunable emission of efficient non-doped organic light-emitting diodes. J Mater Chem C, 2014;2:3416–3428.

[30] Singh R, Dwivedi AK, Singh A, Lin C, Arumugaperumal R, Wei K, Lin H. Exploration of energy modulations in novel RhB-TPE-based bichromophoric materials via interactions of Cu2+ ion under various semiaqueous and micellar conditions. ACS Appl Mater Interfaces 2016;8:6751–6762.

[31] Link S, El-Sayed MA. Size and temperature dependence of the plasmon absorption of colloidal gold nanoparticles. J Phys Chem B. 1999;103:4212-4217.

[32] Hong Y, Lam JWY, Tang B. Aggregation-induced emission: phenomenon, mechanism and applications. Chem Commun 2009;4332–4353

[33] Birks JB. Photophysics of aromatic molecules. London: Wiley; 1970.

[34] Song Z, Fu H, Wang R, Pacheco LA, Wang X, Lin Y, Cheng J. Secondary structures in synthetic polypeptides from N-carboxyanhydrides: design, modulation, association, and material applications. Chem Soc Rev 2018;47:7401–7425.

[35] Wang Z, Ye J, Li J, Bai Y, Zhang W, He W. A novel triple-mode fluorescent pH probe from monomeric emission to aggregation-induced emission. RSC Adv 2015;5:8912-8917.

[36] Song S, Zheng H, Li D, Wang J, Feng H, Zhu Z, Chen Y, Zheng Y. Monomeric emission and aggregate emission of TPE derivatives in the presence of γ□cyclodextrin. Org Lett 2014;16:2170−2173.

[37] Singh R, Wu H, Dwivedi AK, Singh A, Lin C, Putikam R, Lin M, Wu T, Wei K, Lin H. Monomeric and aggregation emissions of tetraphenylethene in a photo-switchable polymer controlled by cyclization of diarylethene and solvent conditions. J Mater Chem C 2017;5:9952-9962.

## Highlights

- A synthetic polypeptide-based amphiphilic bioconjugate bearing tetraphenylethylene (TPE) is synthesized
- The obtained amphiphilic bioconjugate shows both the aggregation-induced emission and the monomer emission of the TPE in the THF/$H_2O$ mixture.
- Conformation of the polypeptide blocks within the bioconjugate is not responsible for the monomer emission of the TPE
- Self-assembled nanoparticles (NPs) of the amphiphilic bioconjugate showing the AIE feature are hard to internalize into HeLa cells